

Supporting Information

A molecular dynamics framework to explore the structure and dynamics of layered double hydroxides

Germán Pérez-Sánchez,^{a,*} Tiago L. P. Galvão,^b João Tedim,^b José R. B. Gomes^a

^aCICECO – Aveiro Institute of Materials, Department of Chemistry, University of Aveiro,
Campus Universitário de Santiago, P-3810-193 Aveiro, Portugal

^bCICECO – Aveiro Institute of Materials, Department of Materials and Ceramic
Engineering, University of Aveiro, Campus Universitário de Santiago, P-3810-193 Aveiro,
Portugal

***Corresponding author:** gperez@ua.pt

Campus Universitário de Santiago, University of Aveiro, Aveiro, Portugal

Tel: +351 234401423; Fax: +351 234401470; E-mail address: gpsquark@gmail.com

Contents:

Table S1 Unit cell parameters optimized by DFT calculations.

Table S2 All of the LJ parameters used in this study.

Table S3 Interatomic distances and angles between metal atoms and hydroxyl groups in MI_{1/2}, MI and MII.

Table S4 Comparison between the main interatomic distances and angles in our MD ZI-III structure with data from experiments and simulations.

Figure S1 Angle probability distribution between the NO₃⁻ and CO₃²⁻ molecule plane in MII and MIII, respectively, and the Mg₂Al metal layer plane after 20 ns of production run.

Figure S2 MD simulation snapshots after 20 ns of production run and the density profiles for all of the MI-III systems.

Figure S3 Detailed view of the basal conformations attained in the MD simulations for MII and MIII systems.

Figure S4 XRD pattern comparison between the MII system obtained in the MD simulation with the experimental sample synthesized in our laboratory.

Figure S5 RDFs of selected atom pairs in MIII in order to compare the interatomic distances between literature data and the MD structure obtained in this work.

Figure S6 XRD pattern comparison between the ZII system obtained in the MD simulation with the experimental sample synthesized in our laboratory.

Figure S7 Angle probability distribution of NO₃⁻ and CO₃²⁻ molecule planes in ZII and ZIII, respectively, with the respect to the Zn₂Al metal layer plane after 20 ns of production run.

Figure S8 MD simulation snapshots after 20 ns of production run for ZI-III systems and the respective density profiles.

Figure S9 XRD pattern comparison between the ZII system immersed in the NaCl water solution obtained in the MD simulation with the experimental sample synthesized in our laboratory.

Figure S10 DFT optimized structures for the MI-MIII (top row) and ZI-ZIII (bottom row) LDH systems in which the unit cells were doubled in z-axis direction to show the basal space.

The model presented in this work for Mg_2Al and Zn_2Al LDH materials is ready to be used with different intercalated anions and the well-known open source software GROMACS for MD simulations. For this purpose, all the necessary parameters and inputs to carry out the MD simulations can be found in the following link: <http://sweet.ua.pt/jrgomes/SELMA/MD-LDH/>

Table S1 Unit cell parameters after a geometry optimization by DFT calculations with cell vectors in Angstrom and angles in degrees.

System	a	b	c	α	β	γ
MI	5.266	4.557	7.920	90.00	102.91	90.00
MII	5.266	9.114	8.957	90.00	101.39	90.00
MIII	10.616	5.308	8.259	101.78	101.78	119.97
ZI	10.616	5.308	8.259	101.54	101.54	119.97
ZII	10.616	5.308	9.516	100.20	100.20	119.97
ZIII	10.616	5.308	8.259	101.78	101.78	119.97

Table S2 Lennard-Jones parameters (well depth, D_0 , and equilibrium interatomic distance, R_0) used in this work. The $C^{(6)}$ and $C^{(12)}$ are the Lennard-Jones parameters used in MIII and ZIII systems according with the geometric mixing rules required in the gromos57a7 force field.

Atom	D_0 (kJ mol ⁻¹)	R_0 (nm)
*Zn	3.00000e-07	6.40900e-01
Al	5.56390e-06	4.79430e-01
Mg	3.77810e-06	5.90900e-01
Hydroxide oxygen	6.50193e-01	3.16557e-01
Hydroxide hydrogen	0.00000e+00	0.00000e+00
N (NO ₃ ⁻)	3.37650e-01	3.05900e-01
O (NO ₃ ⁻)	6.09610e-01	2.77100e-01
$C^{(6)}$ and $C^{(12)}$ redefined LJ parameters in MIII and ZIII systems according to the geometric mixing rules used in gromos54a7 force field: $C_{ij}^{(6)} = \sqrt{(C_{ii}^{(6)} * C_{jj}^{(6)})}$ $C_{ij}^{(12)} = \sqrt{(C_{ii}^{(12)} * C_{jj}^{(12)})}$	$C^{(6)}$ (kJ mol ⁻¹)	$C^{(12)}$ (kJ mol ⁻¹)
*Zn	0.0000000825	0.0000000057
Al	0.0000002703	0.0000000033
Mg	0.0000006433	0.0000000274
Hydroxide oxygen	0.0026170608	0.0000026335
Hydroxide hydrogen	0.0000000000	0.0000000000
C (CO ₃ ⁻)	0.0023406244	4.937284e-06
O (CO ₃ ⁻)	0.0022619536	7.4149321e-07

*New LJ parameters for Zinc obtained in this work.

Table S3 Interatomic distances and angles in our MD MI_{1/2}, MI, MII and MIII structures. The standard deviation (2σ) related to the first maximum of the RDF peak to obtain the interlayer distance in this work is 0.06 Å. The error in the angles are given between brackets.

	MI _{1/2}	MI	II	MIII
	Interatomic distances (Å)			
(Mg,Al)-O _{OH}	2.12	2.12	2.11	2.11
O _{OH} -O _{OH}	2.71	2.71	2.72	2.71
	angles (°)			
O _{OH} -Mg-O _{OH} (inter)	82(5)	81(5)	81(5)	81(5)
O _{OH} -Al-O _{OH} (inter)				
O _{OH} -Al,Mg-O _{OH} (intra)	99(1)	98(1)	98(1)	98(1)

*Inter and intra between brackets means hydroxyl oxygens placed in the same or adjacent hydroxyl layers, respectively.

Table S4. Comparison between the main interatomic distances and angles in our MD ZI-III structure with data from experiments and simulations.¹⁴ O1 is the hydroxyl oxygen atom, O2 oxygen in water molecules, Zn and Al are the zinc and aluminium atoms, respectively. Cl represents chloride ions and C the carbon atom in CO₃²⁻ anions. Distances have been obtained with the RDF profiles. Estimated errors are given between brackets. The standard deviation (2σ) related to the first maximum of the RDF peak to obtain the interlayer distance in this work is 0.06 Å.

	ZI _{1/2}	Literature ¹⁴ (ZI _{1/2})		ZIII	Literature ¹⁴ (ZIII)	
		Calcd.	Expl.		Calcd.	Expl.
Zn-O _{OH}	2.15	2.08	2.015	2.15	2.059	2.003
Al-O _{OH}	2.00	1.97	2.015	2.00	1.963	2.003
Zn-Zn	3.16	3.078	3.074	3.16	3.090	3.076
	5.49	5.321	5.328	5.48	5.335	5.327
Al-Al	5.48	5.316	5.326	5.48	5.317	5.327
Zn-Al	3.16	3.067	3.076	3.16	3.075	3.076
O _{OH} -Cl, C	3.15	3.207	3.030	3.06	3.148	3.386
O _{carbonate} -Cl, C	3.17	3.191	—	3.34	3.161	—
O _{OH} -O _{OH}	2.77	2.75	2.622	2.77	2.756	2.568
O _{OH} -O _{carbonate}	2.77	2.785	2.879	2.69	2.766	2.937
Zn-Cl, C	2.38	2.196	—	2.37	2.225	—
	4.01	4.060	4.004	4.03	4.179	3.790/4.204
Al-Cl, C	4.87	4.792	4.004	4.06	4.215	3.790/4.204
				4.80	4.927	—
Cl-Cl, C-C	4.36	4.312	—	5.69	4.179	—

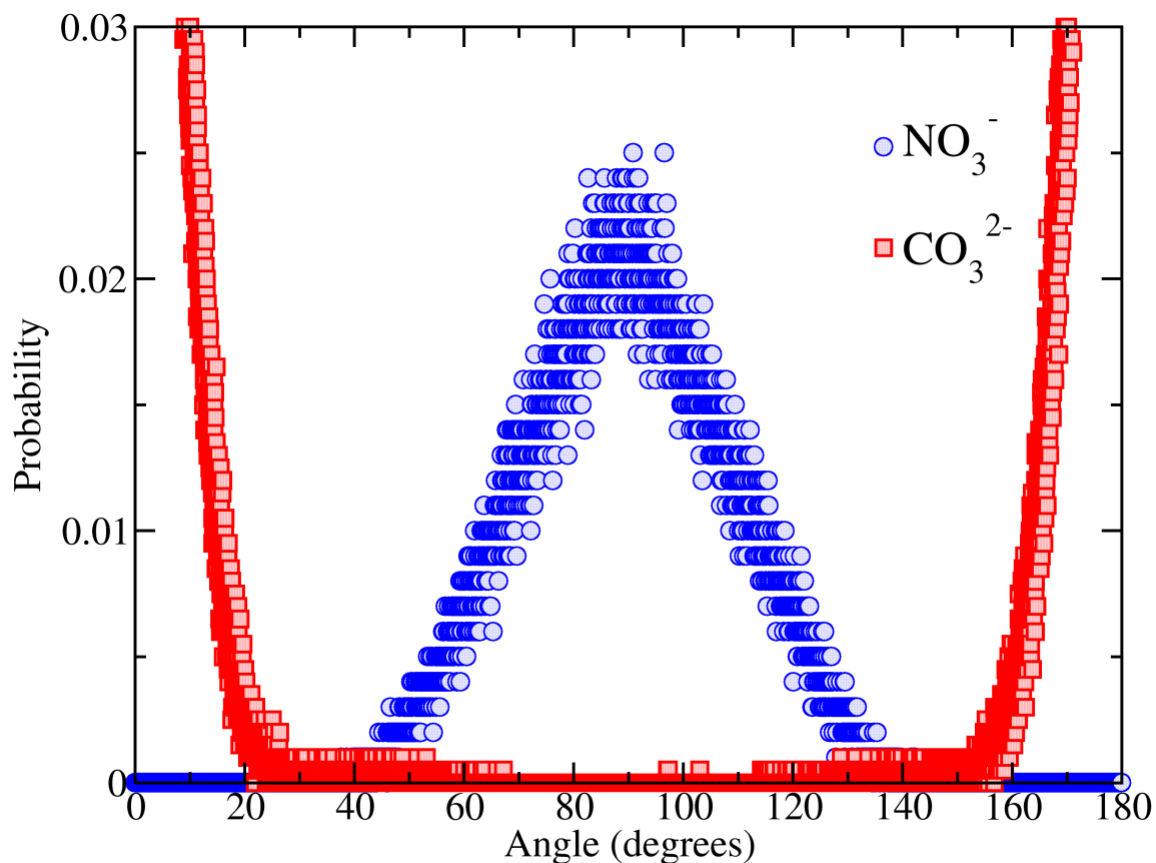


Figure S1. Angle probability distribution of NO_3^- molecule plane (blue circles) and the plane defined by the metal layer in the MII LDH system after 20 ns of NpT production run. The main peak blue shows that 90° is the most likely angle of NO_3^- molecules in the basal space with the respect of the metal plane. Different configuration was obtained for the intercalated carbonates in MIII in which the angle probability distribution of the CO_3^{2-} molecule plane (red squares) shows a preferred angle close to 0° or close to 180° (parallel to the metal layer) respect the metal layer.

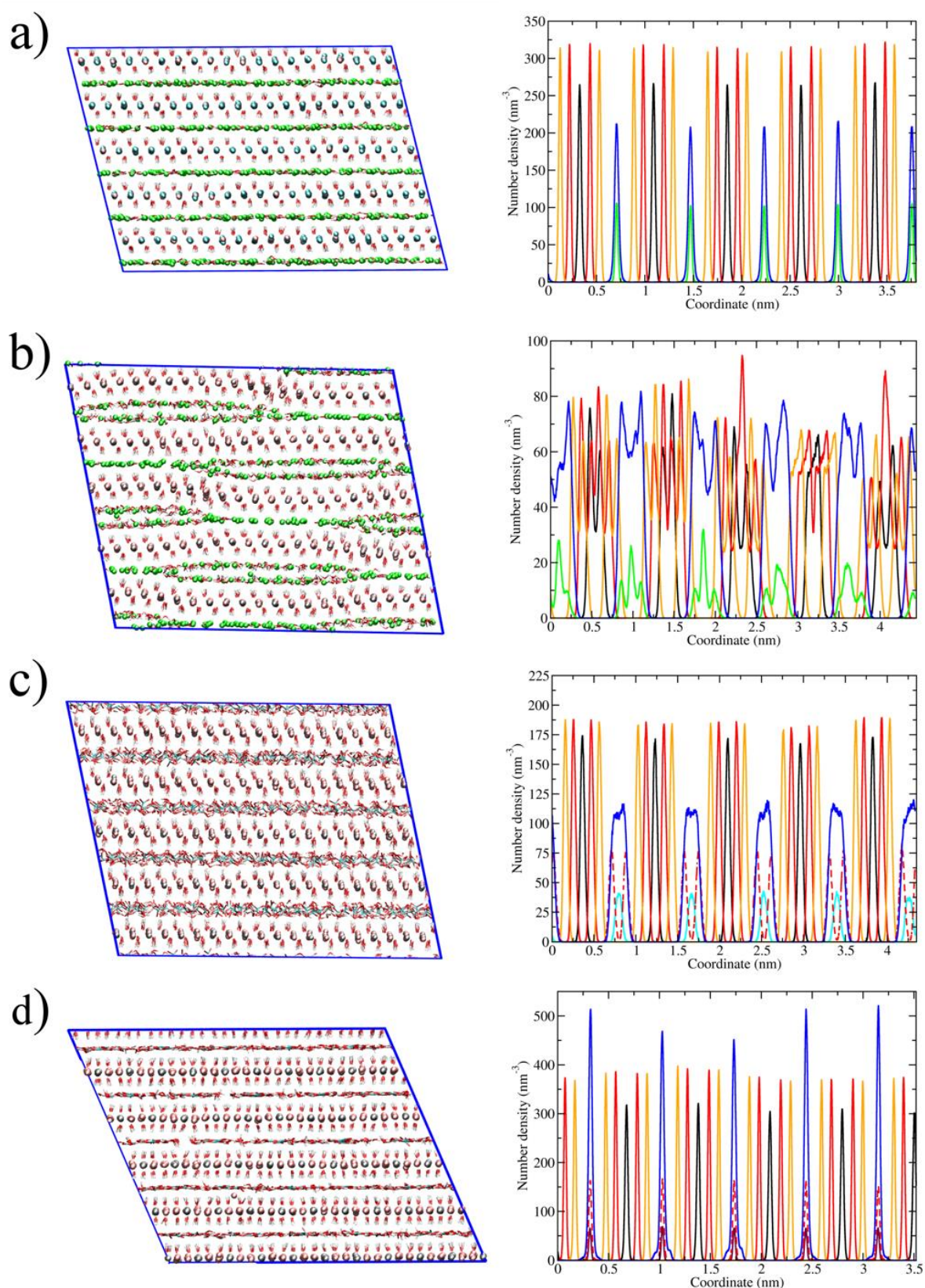


Figure S2. Density profiles of the entire simulation box in the basal direction (normal to the metal layer) obtained for a) $MI_{1/2}$, b) MI, c) MII and d) MIII systems. Simulation snapshots in the left show the obtained configuration after 20 ns of NpT production run. The colour code is as follows: magnesium in pink, aluminium in grey (both in black in the respective density profiles), oxygen in red where the hydroxide oxygen is plotted in solid line but dashed in NO_3^- and CO_3^{2-} anions. Hydroxide hydrogen is in white in the simulation snapshots in the left but in yellow in the density profiles. Chloride anions are in green, nitrate and carbonate atoms are in cyan and ochre, respectively and finally water molecules are in blue.

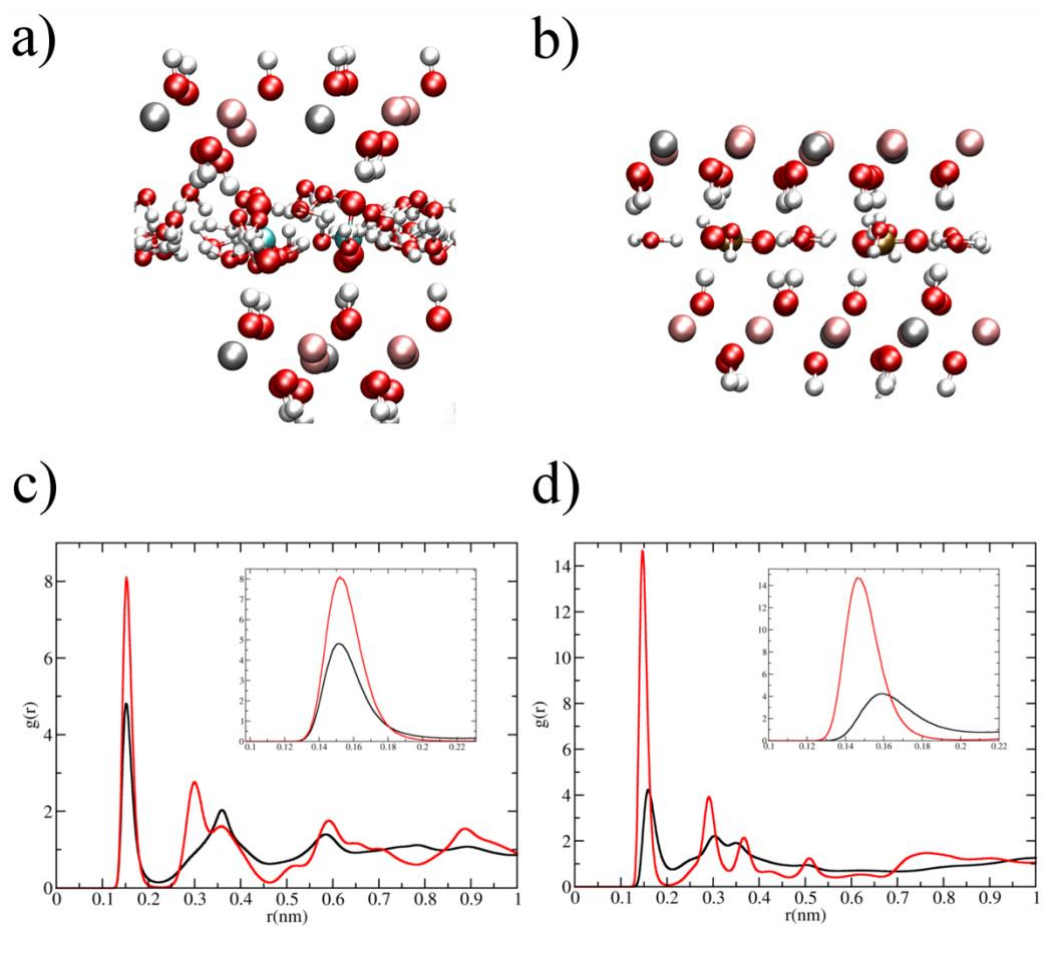


Figure S3. Snapshots showing a detailed view of the basal conformations attained in the MD simulations for a) MII and b) MIII. The water molecules in MII have more available space, thereby, the NO_3^- have less constraints in the movement. Contrary, the interlayer distance in MIII is almost twice smaller than in the MII system. Bearing in mind that the anion size is similar in both, the CO_3^{2-} anions can barely move and the water molecules are constrained between the carbonate anions. c) RDF between anion oxygen atoms and hydroxyl hydrogens of the LDH layer for MII (black) and MIII (red) in order to estimate the H-bonding. d) RDF between anion oxygen atoms and water molecules used to evaluate the arrangement of water molecules around the intercalated anions in MII (black) and MIII (red). Colour code in a) and b) is the same as in Figure S2.

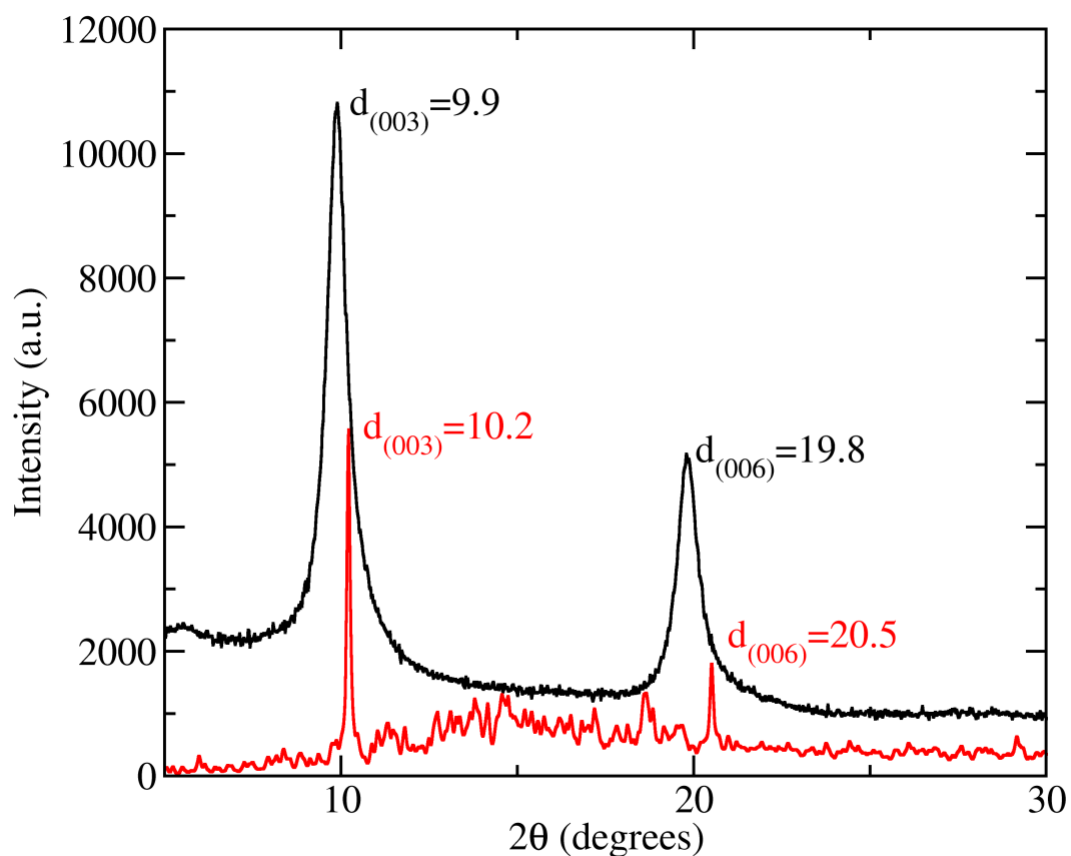


Figure S4. XRD pattern comparison between the MII system obtained in the NpT MD production run after 20 ns (red line) with the synthesized in our laboratory (black line). Both patterns show a reasonable agreement respect the main d_{003} peak whereas d_{006} can be shyly discerned from the signal noise in the MD pattern, being closely to the experimental d_{006} counterpart. In fact, $d_{003} \sim 2 \times d_{006}$ as expected in highly crystallised system. The interlayer distances obtained from d_{003} values in the experimental sample (8.9 Å) and the MD simulation (8.7 Å) are shown Table 3.

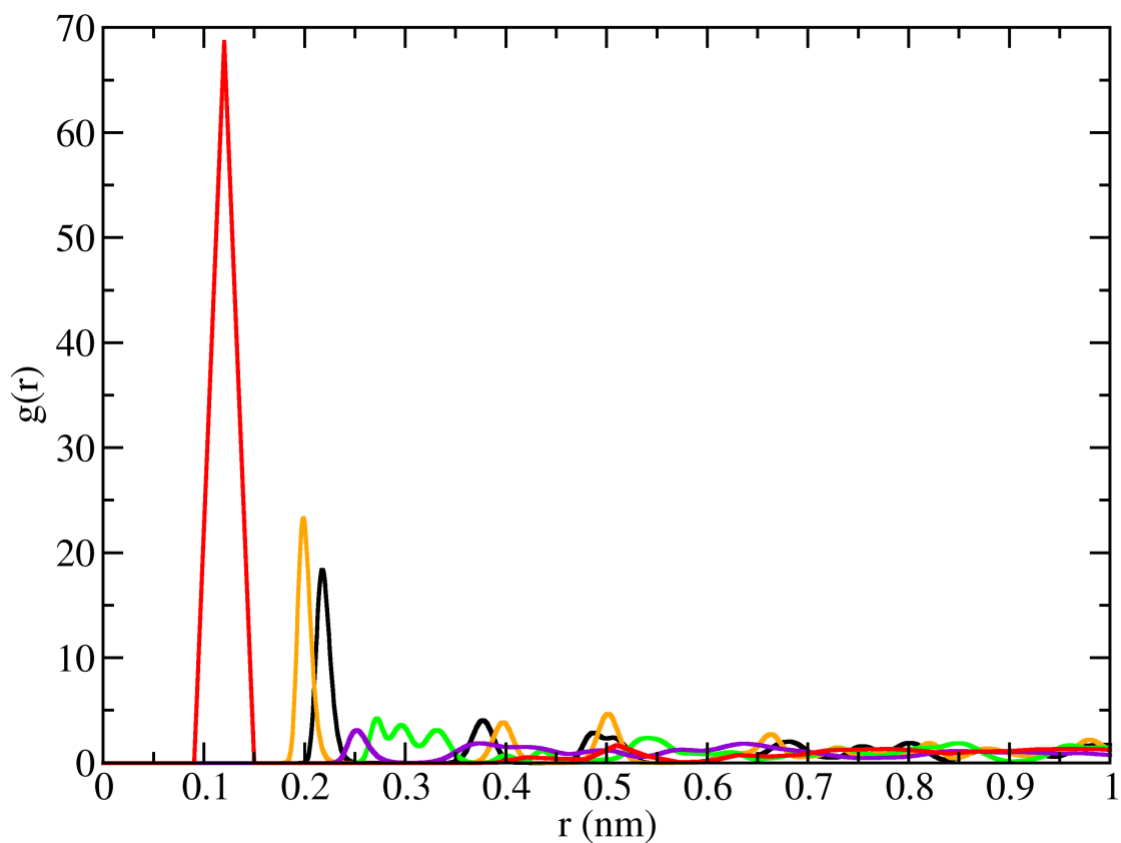


Figure S5. RDFs in MIII used in Table S4 to obtain the interatomic distances of the selected atoms to compare the MD structure with data from the literature. The colour code for each RDF is as follows; Mg-O1 orange, Al-O1 black, O1-O1 green, O1-O2 violet and C-O2 red. The inset in the figure shows in detail the main peaks used to obtain the inter atom distances.

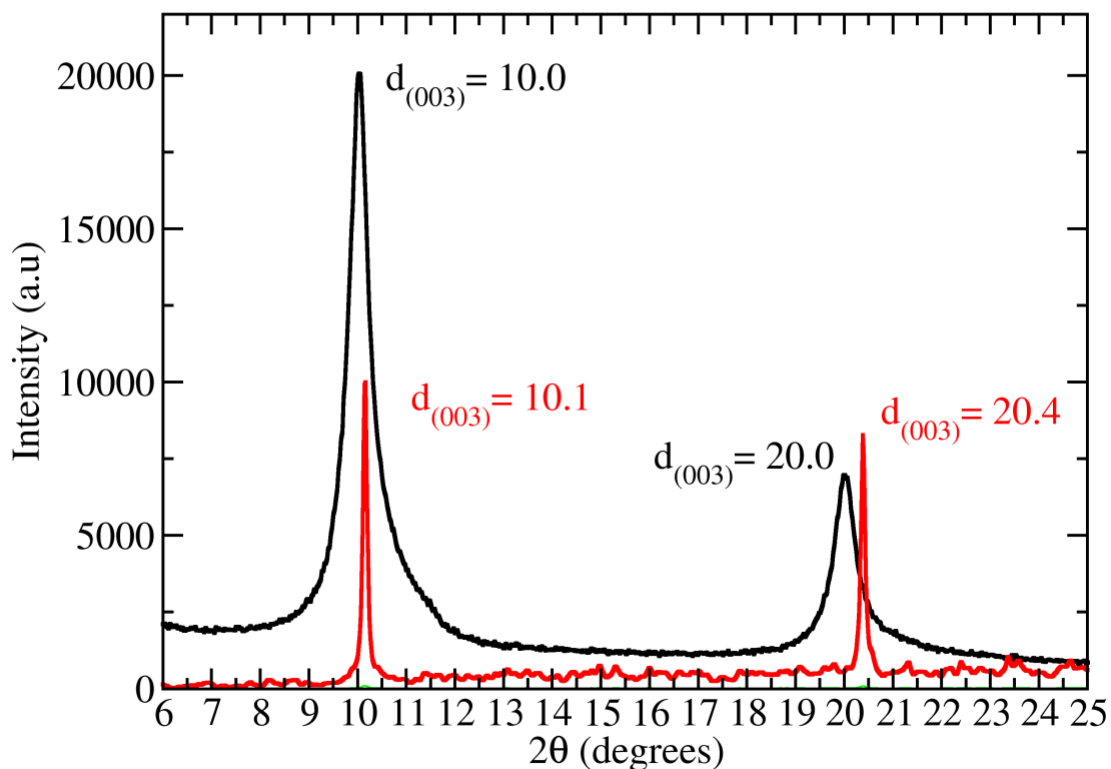


Figure S6. XRD pattern comparison between the ZII system obtained in the NpT MD production run after 20 ns (red line) and the system synthesized in our laboratory (black line). Both patterns show a reasonable agreement between both d_{003} and d_{006} peaks $d_{003} \sim 2 \times d_{006}$ in the experimental and computational sample as expected in highly crystallised system. The interlayer distances obtained from those d_{003} values in the experimental sample (8.8 Å) and the MD simulation (8.7 Å) are shown in Table 6.

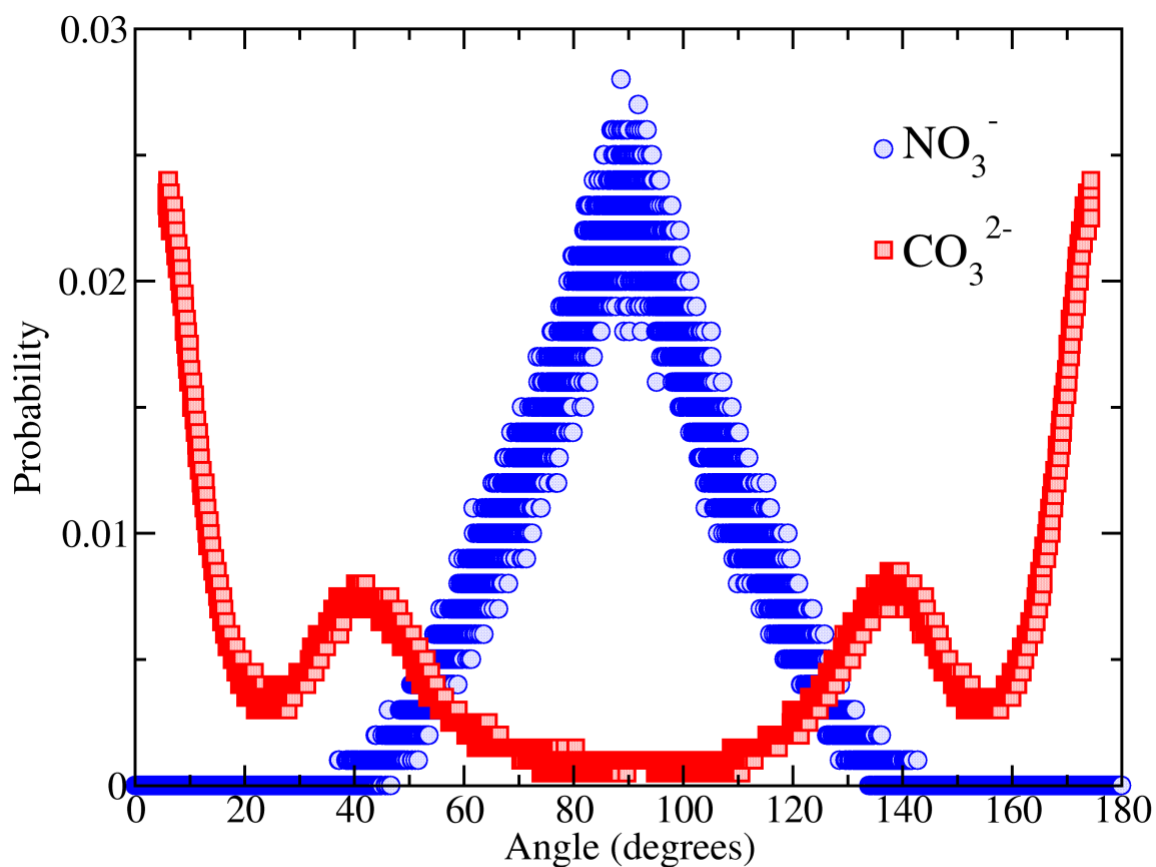


Figure S7. Angle probability distribution of NO_3^- (blue circles) respect the plane defined by the metal layer in the ZII LDH system. The maximum in this distribution shows 90° as the most likely angle between the NO_3^- molecule and the metal layer plane after 20 ns of NpT production run. Different configuration was obtained in ZIII in which the angle probability distribution of CO_3^{2-} molecule plane (red squares) shows a preferred angle close to 0° or 180° besides some of them arranged in tilted angles around 40° and 140° with the respect of the metal layer.

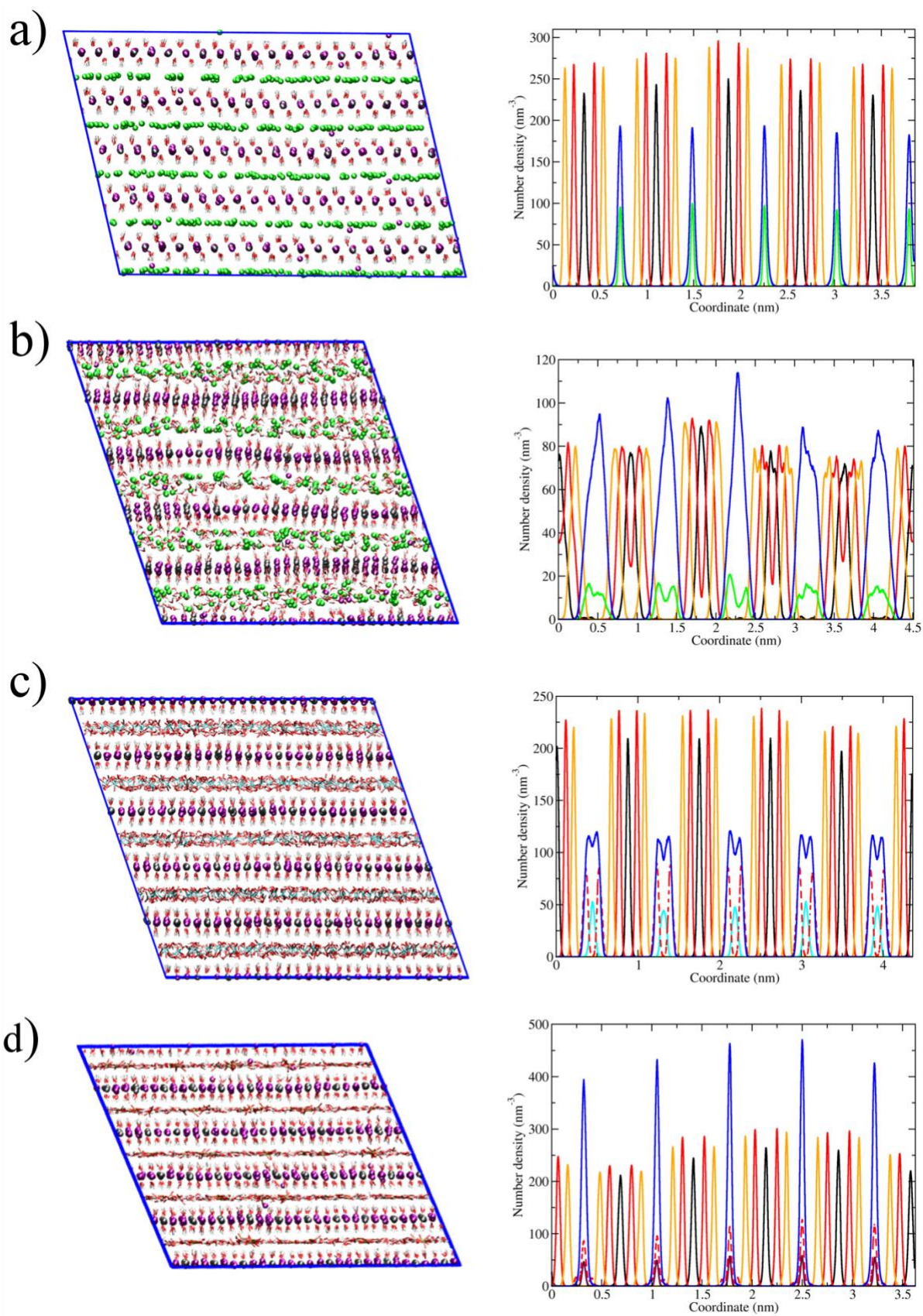


Figure S8. Density profiles of the obtained simulation boxes after 20 ns of NpT production run with the basal direction normal to the metal layer. a) and b) show the ZI system with 1 or 2 water molecules per chloride anion, respectively. c) and d) plot the ZII and ZIII systems, respectively. In the left, the respective density profiles between

two adjacent LDH layers are plotted. The colour code used in the density profiles is the same as Figure S2 but zinc atoms are in purple.

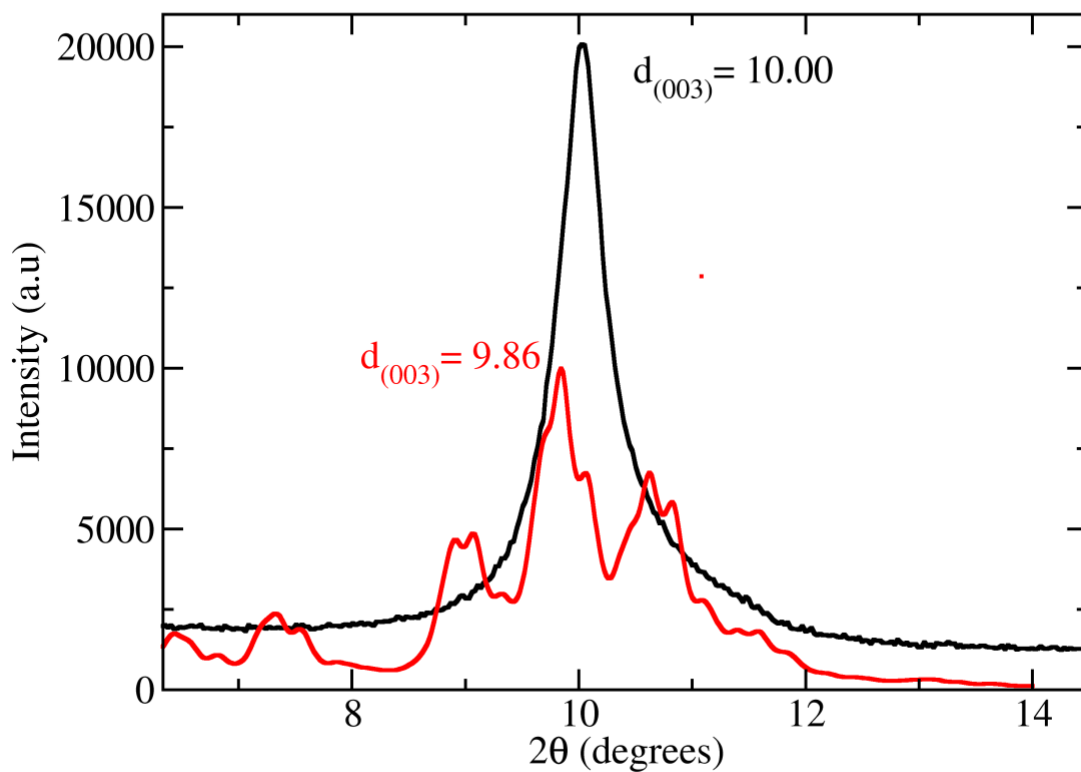


Figure S9. Computed XRD pattern shown in red colour after 20 ns of simulation time for the ZII system immersed in a sodium chloride water solution that mimics one of the experimental applications of such materials in corrosion. The computed pattern is compared with the ZII experimental counterpart synthesized in our laboratory (black line). The interlayer distance obtained from the experimental sample 2θ value ($d_{003}=10.00$) is 8.8 Å, also shown in Table 6, in good agreement with the MD ZII simulated system in solution ($d_{003}=9.86$) 8.9 Å.

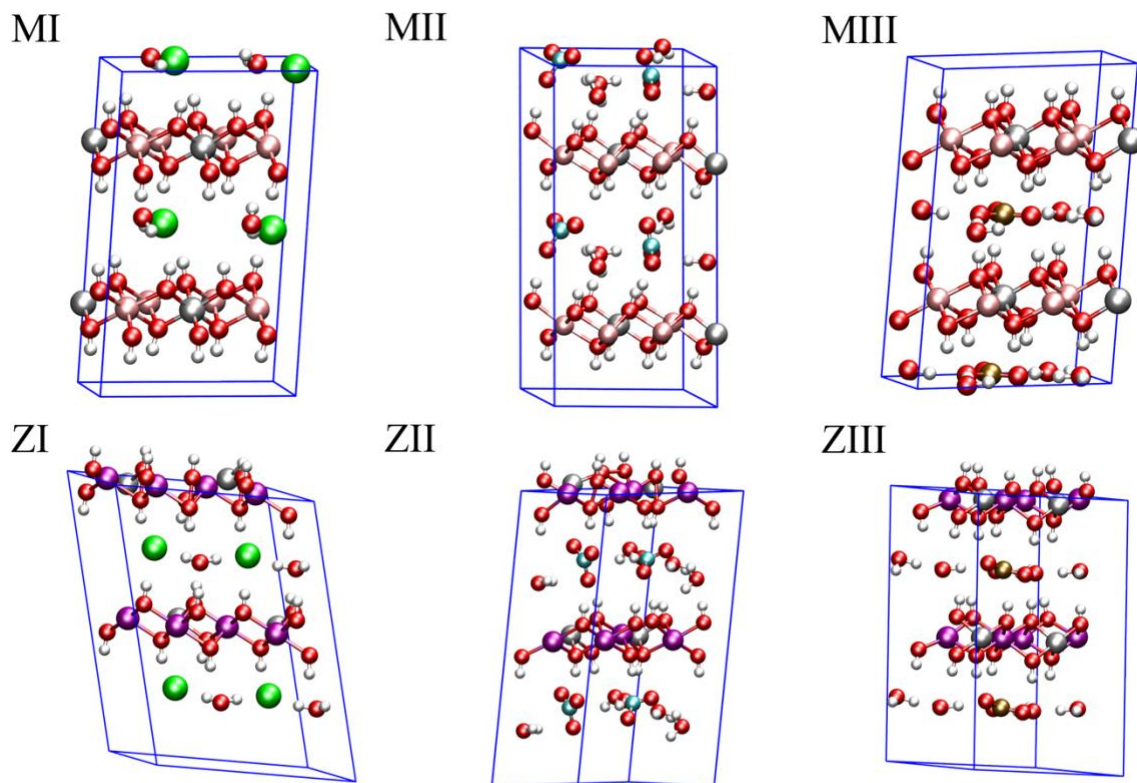


Figure S10. DFT optimized structures for the MI-MIII (top row) and ZI-ZIII (bottom row) LDH systems in which the unit cells were doubled in the z-axis direction to show the basal space. Colour code for spheres: silver is Al; pink is Mg; purple is Zn; green is Cl; cyan is N; ochre is C; red is O; and white is H.